



THE UNIVERSITY *of* EDINBURGH

Edinburgh Research Explorer

A Refined Analytical Model For Externally-Induced Sloshing In Half-Full Deformable Horizontal Cylindrical Liquid Containers.

Citation for published version:

Karamanos, S & Kouka, A 2016, 'A Refined Analytical Model For Externally-Induced Sloshing In Half-Full Deformable Horizontal Cylindrical Liquid Containers.', *Soil Dynamics and Earthquake Engineering*, vol. 85, pp. 191-201. <https://doi.org/10.1016/j.soildyn.2016.03.004>

Digital Object Identifier (DOI):

<http://dx.doi.org/10.1016/j.soildyn.2016.03.004>

Link:

[Link to publication record in Edinburgh Research Explorer](#)

Document Version:

Peer reviewed version

Published In:

Soil Dynamics and Earthquake Engineering

General rights

Copyright for the publications made accessible via the Edinburgh Research Explorer is retained by the author(s) and / or other copyright owners and it is a condition of accessing these publications that users recognise and abide by the legal requirements associated with these rights.

Take down policy

The University of Edinburgh has made every reasonable effort to ensure that Edinburgh Research Explorer content complies with UK legislation. If you believe that the public display of this file breaches copyright please contact openaccess@ed.ac.uk providing details, and we will remove access to the work immediately and investigate your claim.



A REFINED ANALYTICAL MODEL FOR EARTHQUAKE-INDUCED SLOSHING IN HALF-FULL DEFORMABLE HORIZONTAL CYLINDRICAL LIQUID CONTAINERS

Spyros A. Karamanos¹ and Angeliki Kouka

University of Thessaly

Volos 38334, Greece

Keywords: Seismic Response, Liquid Container Excitation, Horizontal-Cylindrical Container, Fluid-Structure Interaction, Sloshing.

ABSTRACT

The coupled response of elastic deformable liquid containers of horizontal-cylindrical shape under external seismic excitation is examined, through an analytical methodology, assuming inviscid-incompressible fluid and irrotational-flow conditions. In particular, the case of a half-full horizontal-cylindrical deformable container is examined, considering an analytical series-type solution for the velocity potential function that describes the liquid motion under external excitation. This mathematical analysis extends the solution methodology presented in previous publications of the senior author, taking into account full coupling between sloshing and wall deformation in a rigorous manner, where wall deformation is considered through a sinusoidal assumed-shape function. In the mathematical formulation, the velocity potential is decomposed into three parts: (a) a first part, which represents liquid motion that follows the external excitation, (b) a “convective part”, representing liquid motion

¹ Corresponding author: skara@mie.uth.gr

associated with free surface elevation (sloshing), and (c) a third part caused by the wall deformation. Using an elegant mathematical manipulation, the coupled transient overall response of the liquid-container system is obtained in an efficient manner. Numerical results are presented in terms of the principal natural frequencies of the coupled system, as well as the system response under strong seismic input, and emphasize on the effects of container aspect ratio on the dynamic behavior of the system. The mathematical formulation for the case of long cylinders results in a simplified model, identical to the simplified “physical model” presented in a previous publication.

1 INTRODUCTION

The presence of a free surface in partially filled liquid containers allows for fluid motions relative to the container, associated with free-surface elevation. This phenomenon, referred to as “liquid sloshing”, is generally caused by external tank excitation, and may have a significant influence on the response of the container. Assuming ideal fluid, the fluid flow is described through a velocity potential function satisfying the Laplace equation within the fluid, the kinematic condition on the tank wall, and the kinematic and dynamic free-surface conditions. Furthermore, considering small amplitude conditions, a linearized condition on the free surface of liquid is obtained. In the absence of external excitation, sloshing can be regarded as an eigenvalue problem, which represents the oscillations of the free surface of an ideal liquid inside a stationary container. The eigen-problem solution provides the natural frequencies of fluid oscillation (sloshing frequencies) and the corresponding sloshing modes, and depends strongly on the shape of the container. In the case of externally excited container, sloshing becomes a transient problem. The total liquid motion can be decomposed in two parts, first part which represents liquid motion that follows the external excitation, and a second part associated with sloshing, which expresses fluid motion with respect to the container. The solution of the transient problem provides the hydrodynamic pressures and forces on the container’s wall.

In non-deformable liquid containers of rectangular and vertical-cylindrical shape, the sloshing problem can be solved analytically, using separation of variables, and the corresponding sloshing modes are mutually orthogonal and uncoupled. For other geometries (e.g. horizontal cylinders or spheres) exact analytical solutions may not be available, and the use of numerical or semi-numerical methods becomes necessary. Sloshing frequencies in non-deformable circular cylinders (canals) as well as the corresponding transient problem of externally-induced sloshing has been studied numerically in an early work by Budiansky (1960), using space transformations to map the initial circular region to a more convenient plane region. The flow field was described by a set of integral equations, which was solved using a Galerkin-type solution. Further contributions on the calculation of sloshing frequencies in horizontal cylindrical containers filled up to an arbitrary height have been reported by Moiseev & Petrov (1966), and later by Fox & Kuttler (1981, 1983), McIver (1989), McIver & McIver (1993), Zhou *et al.* (2008) using numerical or semi-numerical methods.

Recently, the analysis of horizontal cylindrical liquid containers under external excitation has received quite some attention, mainly because of its application in dynamics and stability of moving vehicles containing a liquid with a free surface. Faltinsen & Timokha (2009, 2010) presented a multimodal method for two-dimensional forced liquid sloshing in a circular container, which employs an expansion in terms of the natural sloshing modes. The multimodal method has also been used by Kolaei et al. (2014a, 2014b) to analyse sloshing in a moving horizontal-cylindrical container of both circular and general cross-sectional shape. Furthermore, several semi-numerical and numerical works have been motivated by the response of horizontal cylindrical pressure vessels under seismic loading (Kobayashi *et al.*, 1989; Patkas & Karamanos, 2007; Karamanos *et al.* 2009), whereas the reader is referred to the recent paper by Malhotra (2014) for an important application of this topic in the seismic design of a large-scale horizontal-cylindrical container in the International Thermonuclear Experimental Reactor (ITER), in France.

The particular case of a half-full horizontal cylindrical container offers the possibility for developing an elegant analytical formulation, which can be used as benchmark for verifying numerical methodologies. Evans & Linton (1993) developed a series-type analytical solution of the eigenvalue sloshing problem of a half-full two-dimensional liquid container, expanding the velocity potential in a series of non-orthogonal bounded harmonic spatial functions. This series solution has been extended by the authors (Papasprou *et al.* 2004a, b) for the calculation of hydrodynamic pressures and forces in half-full cylinders under transverse and longitudinal external excitation respectively, expanding the velocity potential in bounded series in terms of arbitrary time functions and their associated non-orthogonal spatial functions, resulting in a system of ordinary linear differential equations. In the case of transverse excitation, a simplified three-dimensional model was also presented by Papasprou *et al.* (2004b) and further developed in Karamanos *et al.* (2006), extending the series solution to account for wall deformation and calculating the coupled response of the liquid-structure system. More recently Hasheminejad & Aghabeigi (2009, 2011) analyzed sloshing in half-full horizontal cylindrical containers of elliptical cross-section and in a subsequent publication they extended their formulation to examine the effects of vertical or horizontal side baffles on sloshing response (Hasheminejad & Aghabeigi, 2012).

The present work, motivated by the seismic analysis of horizontal-cylindrical pressure vessels (Karamanos *et al.*, 2006), is aimed at developing a rigorous mathematical model to calculate sloshing effects in deformable half-full horizontal cylindrical containers under external excitation in the transverse direction, extending and refining the work presented in Papaspyrou *et al.* (2004b). The coupled liquid-structure response is tackled through an analytical methodology, considering the influence of container wall motion on liquid sloshing, through an appropriate assumed shape function to account for vessel deformation. It should be noted that for the case of deformable containers, the “sloshing” or “convective” motion has been customarily considered neglecting wall deformation effects. Such an approach has been used extensively in the seismic analysis of vertical cylindrical liquid storage tanks, where the container’s deformation was taken into account through either simple assumed-shape functions (Veletsos & Yang 1977, Fischer 1979), or more elaborate shell deformation models (Haroun 1983, Natsiavas 1988, Gupta 1995). In the present work, the case of half-full horizontal cylinders under external transverse excitation is examined using a mathematical formulation that allows for full coupling between liquid motion and wall deformation through an explicit and rigorous manner. A similar approach has been followed by Fischer & Rammerstorfer (1999) for the case of upright cylindrical liquid containers. The formulation decomposes the motion in three parts: a first part that follows the external source, a second part due to container deformation and a third part associated with sloshing of the liquid free surface. In the present study, following the terminology widely adopted in the literature for earthquake response of liquid storage tanks (e.g. Veletsos & Yang, 1977; Fischer, 1979; and Fischer & Rammerstorfer, 1999), these three parts are referred to as “impulsive” motion, “deformation” motion and “convective” motion respectively.

A truncated solution is also developed considering only the first two terms of the series in the transverse direction, which yields an elegant solution of good accuracy and enables the parametric study. The particular case of harmonic excitation is also examined, which results in a system of algebraic equations. Comparison of the present rigorous approach with the more simplified approach proposed by Papaspyrou *et al.* (2004b) is conducted towards better understanding the effects of container wall deformation on the overall dynamic response of the half-full horizontal cylinder. The numerical results are presented in terms of the frequencies of the coupled system with respect to the aspect ratio of the container, as well as the response the liquid-

container system under external excitation from a severe seismic event for different values of the aspect ratio.

2 FORMULATION OF THE COUPLED PROBLEM

The fluid is contained in a half-full horizontal cylindrical vessel of radius R , with the y -axis of the coordinate system x,y,z , where axis y points vertically downwards (Figure 1). The geometry is described in terms of the cylindrical coordinates r, θ, z .

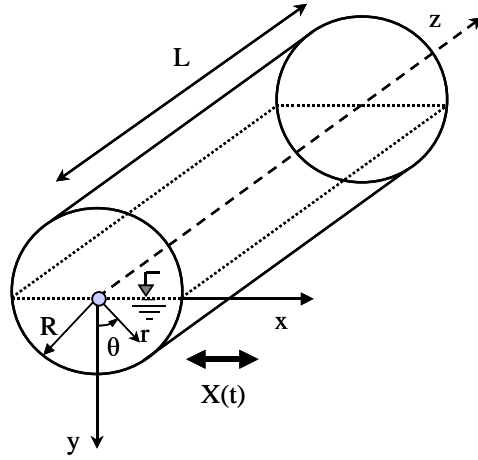


Figure 1: Schematic representation of the problem: half-full horizontal cylindrical container and coordinate system.

2.1 Vessel deformation

The container undergoes an arbitrary motion of its supports in the direction of the x axis with displacement $X(t)$. The vessel is assumed flexible (deformable) in the form of a beam-type deformation where the cross-section remains circular (those vessels are rather thick to resist high internal pressure). However, relatively long horizontal cylindrical vessels ($L/R \geq 10$), quite common in petrochemical industries and refineries, exhibit a beam-type deformation, which may affect the overall response under transverse excitation. Thus, neglecting local (shell-type) modes, while the cylinder cross-section remains circular (undeformed) due to its significant thickness, the motion of the cylindrical container is directly determined by the motion of the cylinder axis, which is decomposed in two parts (Figure 2), the motion of the supports

$X(t)$, independent of z coordinate, and the motion due to the deformation of the container described by a function $y(z, t)$

$$y(z, t) = \psi(z) \Delta(t) \quad (1)$$

where $\psi(z)$ is an assumed shape function and $\Delta(t)$ is an unknown degree of freedom that represents the magnitude of container motion relative to the supports.

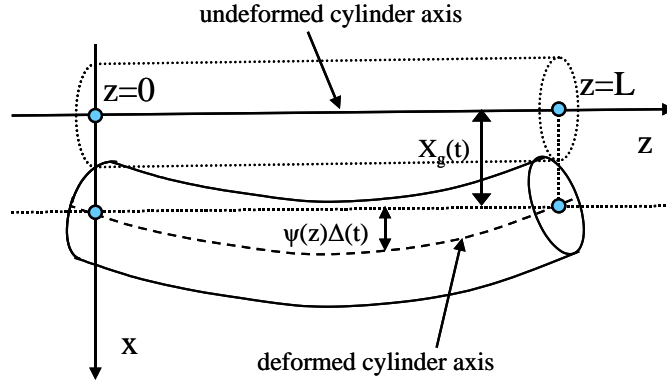


Figure 2: Beam-type deformation of horizontal cylinder, simply supported at $z = 0$ and $z = L$.

2.2 Fluid motion and decomposition

Assuming inviscid-incompressible fluid and irrotational flow conditions, the flow is described by a velocity potential function $\Phi(r, \theta, z, t)$, which satisfies Laplace equation within the fluid volume, with appropriate boundary conditions on the container's wall and the free surface of the liquid. The velocity potential $\Phi(r, \theta, z, t)$, satisfies Laplace equation within the domain $r < R$, $-\pi/2 < \theta < \pi/2$, $0 < z < L$

$$\nabla^2 \Phi = \frac{1}{r} \frac{\partial \Phi}{\partial r} + \frac{\partial^2 \Phi}{\partial r^2} + \frac{1}{r^2} \frac{\partial^2 \Phi}{\partial \theta^2} + \frac{\partial^2 \Phi}{\partial z^2} = 0 \quad (2)$$

and the associated boundary conditions at the moving container and the liquid free-surface:

$$\frac{\partial \Phi}{\partial z} = 0 \quad z = 0, L, \quad -\pi/2 < \theta < \pi/2, \quad 0 < r < R \quad (3)$$

$$\frac{\partial \Phi}{\partial r} = (\dot{X} + \psi(z) \dot{\Delta}) \sin \theta \quad r = R, \quad -\pi/2 < \theta < \pi/2, \quad 0 < z < L \quad (4)$$

$$\frac{\partial^2 \Phi}{\partial t^2} \pm \frac{g}{r} \frac{\partial \Phi}{\partial \theta} = 0 \quad \theta = \pm \pi/2, \quad r < R, \quad 0 < z < L \quad (5)$$

Equation (3) is the homogeneous Neumann condition at the two cylinder ends, and equation (4) is the nonhomogeneous Neumann condition at the “wet wall” of the container, expressing that liquid velocity normal to the container wall should be equal to the corresponding velocity of the container. Furthermore, equation (5) is the linearized combined kinematic-dynamic condition at the liquid free surface (e.g. Fischer and Rammerstorfer, 1999; Papaspyrou *et al.* 2004b)

The velocity potential Φ is decomposed in three parts

$$\Phi(r, \theta, z, t) = \varphi_I(r, \theta, t) + \varphi_D(r, \theta, z, t) + \varphi_C(r, \theta, z, t) \quad (6)$$

where $\varphi_I(r, \theta, t)$, $\varphi_D(r, \theta, z, t)$ and $\varphi_C(r, \theta, z, t)$ are the so-called “impulsive”, “deformation” and “convective” potentials respectively, following the terminology widely adopted in the literature for the seismic response of liquid storage containers. More details on this decomposition procedure can be found in the paper by Fischer and Rammerstorfer (1999).

The impulsive motion potential φ_I satisfies the Laplace equation within the liquid volume

$$\nabla^2 \varphi_I = 0 \quad r < R, \quad -\pi/2 < \theta < \pi/2 \quad (7)$$

and the following boundary conditions

$$\frac{\partial \varphi_I}{\partial r} = (\dot{X} + \psi_m \dot{\Delta}) \sin \theta \quad r = R, \quad -\pi/2 < \theta < \pi/2 \quad (8)$$

$$\varphi_I = 0 \quad \theta = \pm \pi/2, \quad r < R \quad (9)$$

In Equation (8), ψ_m is the mean value of $\psi(z)$:

$$\psi_m = \frac{1}{L} \int_0^L \psi(z) dz \quad (10)$$

so that

$$\psi(z) = \psi_m + \tilde{\psi}(z) \quad (11)$$

and

$$\int_0^L \tilde{\psi}(z) dz = 0.$$

From Equations (7) - (9), one readily concludes that the impulsive potential is two-dimensional, independent of the z coordinate.

The “deformation” potential φ_D satisfies the Laplace equation in the liquid volume

$$\nabla^2 \varphi_D = 0 \quad r < R, \quad -\pi/2 < \theta < \pi/2, \quad 0 < z < L \quad (12)$$

and the following boundary conditions:

$$\frac{\partial \varphi_D}{\partial z} = 0 \quad z = 0, L, \quad -\pi/2 < \theta < \pi/2, \quad 0 < r < R \quad (13)$$

$$\frac{\partial \varphi_D}{\partial r} = \dot{\Delta} \tilde{\psi}(z) \sin \theta \quad r = R, \quad -\pi/2 < \theta < \pi/2, \quad 0 < z < L \quad (14)$$

$$\varphi_D = 0 \quad \theta = \pm\pi/2, \quad r < R, \quad 0 < z < L \quad (15)$$

Finally, the convective potential φ_C , associated with the sloshing motion of the liquid, satisfies the Laplace equation

$$\nabla^2 \varphi_C = 0 \quad r < R, \quad -\pi/2 < \theta < \pi/2, \quad 0 < z < L \quad (16)$$

and the following boundary conditions

$$\frac{\partial \varphi_C}{\partial z} = 0 \quad z = 0, L, \quad -\pi/2 < \theta < \pi/2, \quad 0 < r < R \quad (17)$$

$$\frac{\partial \varphi_C}{\partial r} = 0 \quad r = R, \quad -\pi/2 < \theta < \pi/2, \quad 0 < z < L \quad (18)$$

$$\frac{\partial^2 \varphi_C}{\partial t^2} \pm \frac{g}{r} \frac{\partial \varphi_C}{\partial \theta} = \mp \frac{g}{r} \frac{\partial \varphi_I}{\partial \theta} \mp \frac{g}{r} \frac{\partial \varphi_D}{\partial \theta} \quad \theta = \pm\pi/2, \quad r < R, \quad 0 < z < L \quad (19)$$

In boundary condition (19), the first term on the right-hand side represents the influence of impulsive motion on the convective potential, whereas the second term expresses the influence of vessel deformation on the convective potential.

3 ANALYTICAL SOLUTION

In each of the three problems, the unknown potential is expanded in terms of non-orthogonal (in the transverse direction) bounded harmonic functions and the unknown coefficients of the expansion are determined by satisfying the boundary

conditions. It is easily deduced from the boundary conditions of all three problems and the symmetry of the vessel geometry with respect to planes $z=L/2$ and $\theta=0$, that all solutions must be symmetric in terms of z and antisymmetric in terms of θ , with respect to the $z=L/2$ and $\theta=0$ planes respectively. Therefore, in all cases, a general solution is considered in a series form that satisfies the Laplace equation, as described in the following paragraphs.

3.1 Analytical solution for the fluid potential

The solution of the two-dimensional impulsive problem is written in the following series form in terms of two-dimensional cylindrical harmonics

$$\varphi_I(r, \theta) = \sum_{n=1}^{\infty} \dot{q}_n^I(t) r^n \sin(n\theta) \quad (20)$$

where $\dot{q}_n^I(t)$, $n=1,2,3,\dots$ are generalized coordinates of the impulsive fluid motion. Introducing into the free surface condition (9), one readily obtains that the odd terms should vanish $\dot{q}_{2n-1}^I(t)=0$. Subsequently, introducing into the lateral wall condition (8) one readily obtains the following set of algebraic equations

$$[\mathbf{M}^I] \{\dot{q}^I\} = \{\gamma^I\} [\dot{X} + \psi_m \dot{\Delta}] \quad (21)$$

where

$$\{\dot{q}^I\} = [\dot{q}_2^I \dots \dot{q}_{2n}^I \dots]^T \quad (22)$$

are the unknown even coefficients to be determined,

$$\mathbf{M}_{nm}^I = R^{2n-1} \left(\frac{n^2(-1)^{n+m}}{(n^2 - (m-1/2)^2)} \right) \quad (23)$$

and

$$\gamma^I = [\pi/4 \dots 0 \dots 0]^T \quad (24)$$

The solution of the three-dimensional deformation potential is sought in the form of three-dimensional cylindrical harmonics

$$\varphi_D(r, \theta, z) = \sum_{p=2,4,\dots}^{\infty} \sum_{n=1,2,\dots}^{\infty} \dot{q}_{n,p}^D(t) I_n(k_p r) \sin(n\theta) \cos(k_p z) \quad (25)$$

where $k_p = p\pi/L$, $q_{n,p}^D(t)$ are the generalized coordinates of the deformation motion, and $I_n(\cdot)$ is the modified Bessel function of the first kind. The above expression is substituted first in the free-surface condition (15) to obtain that the odd terms are zero ($q_{2n-1,p}^D(t)=0$, $n=1,2,3,\dots$). Subsequently, application of the lateral-wall condition (14) results in the following set of algebraic equations

$$[\mathbf{M}_p^D] \{\dot{q}_p^D\} = \{\gamma_p^D\} \dot{\Delta} \quad (26)$$

where

$$\{\dot{q}_p^D\} = [\dot{q}_{2,p}^D \dots \dot{q}_{2n,p}^D \dots]^T \quad (27)$$

$$\mathbf{M}_{mn,p}^D = \frac{k_p L}{4} I'_{2n}(k_p R) \left(\frac{n(-1)^{n+m}}{n^2 - (m-1/2)^2} \right) \quad (28)$$

$$\gamma_p^D = [\pi/4 \dots 0 \dots 0]^T \int_0^L \cos(k_p z) \tilde{\psi}(z) dz \quad (29)$$

Finally, the convective potential is written in the following series form, separating even and odd terms:

$$\begin{aligned} \varphi_C(r, \theta, z, t) = & \sum_{n=1}^{\infty} \left[\dot{q}_{2n-1}^C(t) r^{2n-1} \sin[(2n-1)\theta] + \dot{q}_{2n}^C(t) r^{2n} \sin(2n\theta) \right] + \\ & + \sum_{p=2,4}^{\infty} \sum_{n=1}^{\infty} \left[\dot{q}_{2n-1,p}^C(t) I_{2n-1}(k_p r) \sin[(2n-1)\theta] + \dot{q}_{2n,p}^C(t) I_{2n}(k_p r) \sin(2n\theta) \right] \cos(k_p z) \end{aligned} \quad (30)$$

The above expression is introduced in the free surface condition (19) to obtain

$$\dot{q}_{2n}^C(t) = \frac{1}{2ng} \ddot{q}_{2n-1}^C(t) - \dot{q}_{2n}^I(t) \quad n=1,2,3,\dots \quad (31)$$

$$\ddot{q}_{2n-1,p}^C(t) = \frac{k_p g}{2} \left[q_{2n,p}^C(t) + q_{2n-2,p}^C(t) + q_{2n,p}^D(t) + q_{2n-2,p}^D(t) \right] \quad n=1,2,3,\dots, p=2,4,6,\dots \quad (32)$$

$$q_{0,p}^C = q_{0,p}^D = 0 \quad (33)$$

Subsequently, introducing the above expression into the general solution equation (30), and substituting into equation (18) the following set of algebraic systems of equations (34) and (35) is obtained:

$$[\mathbf{M}^C] \{\ddot{q}^C\} + [\mathbf{K}^C] \{q^C\} = \{\gamma^C\} [X + \psi_m \Delta] \quad (34)$$

and

$$[\mathbf{M}_p^C] \{\ddot{\mathbf{q}}_p^C\} + [\mathbf{K}_p^C] \{\mathbf{q}_p^C\} = -[\mathbf{K}_p^C] \{\mathbf{q}_p^D\} \quad (35)$$

where

$$\mathbf{M}_{mn}^C = \mathbf{R}^{2n-1} \left(\frac{2n (-1)^{n+m}}{(n^2 - (m - \frac{1}{2})^2)} \right) \quad (36)$$

$$\mathbf{K}_{mm}^C = (2m-1) \pi g \mathbf{R}^{2m-2} \quad (37)$$

$$\gamma^C = [\pi g \dots 0 \dots 0]^T \quad (38)$$

$$\mathbf{M}_{mn,p}^C = \mathbf{k}_p \mathbf{I}'_{2n}(\mathbf{k}_p \mathbf{R}) \left(\frac{n(-1)^{m+n}}{2(n^2 - (m - \frac{1}{2})^2)} \right) \quad (39)$$

$$\mathbf{K}_{mn,p}^C = \frac{\mathbf{k}_p^2 \pi g}{8} \left[\mathbf{I}'_{2n-1}(\mathbf{k}_p \mathbf{R}) \delta_{m,n} + \mathbf{I}'_{2n+1}(\mathbf{k}_p \mathbf{R}) \delta_{m,n+1} \right] \quad (40)$$

and

$$\{\mathbf{q}^C\} = [\mathbf{q}_1^C \dots \mathbf{q}_{2n-1}^C \dots] \quad (41)$$

$$\{\mathbf{q}_p^C\} = [\mathbf{q}_{2,p}^C \dots \mathbf{q}_{2n,p}^C \dots] \quad (42)$$

$$\{\mathbf{q}_p^D\} = [\mathbf{q}_{2,p}^D \dots \mathbf{q}_{2n,p}^D \dots] \quad (43)$$

Note that parameters $\mathbf{q}_{2n,p}^D$ are given in terms of Δ from equation (26).

Finally, it is important to note that the odd terms $\mathbf{q}_{2n-1,p}^C$ can be directly expressed in terms of the even terms $\mathbf{q}_{2n,p}^C$, substituting the convective solution (30) directly into the lateral wall condition (18), to obtain

$$(2m-1)\mathbf{R}^{2m-2} \dot{\mathbf{q}}_{2m-1}^C = - \sum_{n=1,2,\dots}^{\infty} \mathbf{R}^{2n-1} \frac{n^2 (-1)^{m+n}}{n^2 - (m^2 - 1/2)} \dot{\mathbf{q}}_{2n}^C \quad (44)$$

$$\mathbf{I}'_{2m-1}(\mathbf{k}_p \mathbf{R}) \dot{\mathbf{q}}_{2m-1,p}^C(t) = - \sum_{n=1,2,\dots}^{\infty} \mathbf{I}'_{2n}(\mathbf{k}_p \mathbf{R}) \frac{n(-1)^{m+n}}{2[n^2 - (m^2 - 1/2)]} \dot{\mathbf{q}}_{2n,p}^C(t) \quad (45)$$

3.2 Liquid-container interaction

For each one of the above potentials ϕ_i , $i = I, D, C$, the corresponding pressure of the fluid is computed through Bernoulli's equation

$$p_i = -\rho \frac{\partial \phi_i}{\partial t} \quad (46)$$

where $i = I, D, C$. Conducting an appropriate integration of pressure p_i ($i = I, D, C$) around the lateral surface of the container at a specific section of the cylinder, one obtains the liquid force f_i ($i = I, D, C$) per unit length along the cylinder for the potential under consideration. More specifically, the forces per unit length (along the cylinder) due to “impulsive”, “deformation” and “convective” motion are

$$f_I = -\rho \sum_{n=1}^{\infty} L_{2n}^I \ddot{q}_{2n}^I(t) \quad (47)$$

$$f_D = -\rho \sum_{p=2,4}^{\infty} \sum_{n=1,2}^{\infty} L_{2n,p}^D \cos(k_p z) \ddot{q}_{2n,p}^D(t) \quad (48)$$

$$f_C = -\rho \sum_{p=0,2,4}^{\infty} \sum_{n=1,2}^{\infty} \left[L_{2n-1,p}^C \ddot{q}_{2n-1,p}^C(t) + L_{2n,p}^D \cos(k_p z) \ddot{q}_{2n,p}^C(t) \right] \quad (49)$$

respectively, where L_{2n}^I , $L_{2n,p}^D$, $L_{2n-1,p}^C$, $L_{2n,p}^C$ depend on the cylinder radius R . Thus, the total force per unit length due to the motion of the fluid is

$$f_T(z,t) = f_I(t) + f_D(z,t) + f_C(z,t) \quad (50)$$

Equilibrium of the beam-like cylinder requires that

$$EI \left(\frac{\partial^4 y}{\partial z^4} \right) + m_{SH} \left(\frac{\partial^2 y}{\partial t^2} + \ddot{X} \right) = f_T(z,t) \quad (51)$$

where EI is the bending stiffness of the beam-like cylinder, calculated approximately as follows

$$EI \cong E\pi(R + h/2)^3 h \quad (52)$$

and m_{SH} is the container's mass per unit length. Using an arbitrary admissible function $w(z)$, and assuming that the cylinder is simply supported at two symmetric supports, the weak form of the above equilibrium equation is obtained

$$\int_0^L EI y''(z,t) w''(z) dz + m_{SH} \int_0^L [y(z,t) + \ddot{X}] w(z) dz = \int_0^L f_T w(z) dz \quad (53)$$

In the context of a Galerkin-type solution procedure, the trial function is approximated as

$$w(z) = A_w \psi(z) \quad (54)$$

where A_w is an arbitrary number. Therefore, the following dynamic equilibrium equation is obtained

$$K_b \Delta = \int_0^L f_T \psi(z) dz \quad (55)$$

or

$$\begin{aligned} K_b \Delta = & \int_0^L f_I \psi(z) dz + \int_0^L f_D \psi(z) dz + \\ & + \int_0^L f_C \psi(z) dz - \ddot{\Delta} \left[m_{SH} \int_0^L \psi^2(z) dz \right] - \ddot{X} \left[m_{SH} \int_0^L \psi(z) dz \right] \end{aligned} \quad (56)$$

where

$$K_b = \int_0^L EI \psi''^2(z) dz \quad (57)$$

is the equivalent bending stiffness of the vessel.

4 A TRANSVERSELY-TRUNCATED SOLUTION

It is possible to obtain an elegant solution of the coupled problem, considering only the first two terms in the previous expansions (20), (25) and (30), in terms of θ . This solution can be used for a detailed examination of the effects of wall deformation on the dynamic response. For simplicity, the mass of the container m_{SH} is assumed small and it is neglected.

4.1 Solution for the “impulsive” and “deformation” motions

Using a truncation with the first two terms of θ , the impulsive motion potential in Equations (20) - (24) reduces to the following expression

$$\varphi_1(r, \theta, t) = \frac{3\pi}{16R} (\dot{X} + \psi_m \dot{\Delta}) r^2 \sin 2\theta \quad (58)$$

The corresponding expression for “impulsive” pressure becomes

$$P_I = -\rho \frac{\partial \phi_I}{\partial t} = -\rho \frac{3\pi R}{16} (\ddot{X} + \psi_m \ddot{\Delta}) \sin 2\theta \quad (59)$$

and a simple integration on the lateral surface gives the impulsive force per unit length

$$f_I = -\rho \frac{\pi R^2}{4} (\ddot{X} + \psi_m \ddot{\Delta}) = -\frac{m_L}{2} (\ddot{X} + \psi_m \ddot{\Delta}) \quad (60)$$

Furthermore, the deformation motion potential in Equations (25) - (29) becomes

$$\phi_D(r, \theta, z) = \sum_{p=2,4}^{\infty} \dot{q}_{2,p}^D(t) I_2(k_p r) \sin(2\theta) \cos(k_p z) \quad (61)$$

where

$$\dot{q}_{2,p}^D(t) = \frac{3\pi \dot{\Delta}}{4L k_p I_2'(k_p R)} \int_0^L \tilde{\psi}(z) \cos(k_p z) dz \quad (62)$$

The pressure associated with this potential is given by the following expression

$$P_D = -\rho \sum_{p=2,4}^{\infty} \frac{3\pi}{4L k_p} \frac{I_2(k_p R)}{I_2'(k_p R)} \ddot{\Delta} \left(\int_0^L \cos(k_p z) \tilde{\psi}(z) dz \right) \sin 2\theta \cos(k_p z) \quad (63)$$

and the corresponding force per unit length is

$$f_D = -\rho \sum_{p=2,4}^{\infty} \frac{\pi R}{L k_p} \frac{I_2(k_p R)}{I_2'(k_p R)} \ddot{\Delta} \left(\int_0^L \cos(k_p z) \tilde{\psi}(z) dz \right) \cos(k_p z) \quad (64)$$

4.2 Solution for “convective” motion and liquid-vessel interaction

Considering only the first two terms in the series solution (30), and using the fact that Equations (44) - (45) reduce to

$$q_2^C = -\frac{3\pi}{16R} q_1^C \quad (65)$$

$$q_{2,p}^C = -\frac{3\pi}{8} \frac{I_1'(k_p R)}{I_2'(k_p R)} q_{1,p}^C \quad (66)$$

respectively, the convective motion potential from Equation (30) and the corresponding pressure, written in terms of variables q_1^C and $q_{1,p}^C$ become

$$\begin{aligned} \varphi_C(r, \theta, z, t) = & \dot{q}_1^C(t) \left[r \sin\theta - \frac{3\pi}{16R} r^2 \sin 2\theta \right] + \\ & + \sum_{p=2,4}^{\infty} \dot{q}_{1,p}^C(t) \left[I_1(k_p r) \sin\theta - \frac{3\pi}{8} \frac{I_1'(k_p R)}{I_2'(k_p R)} I_2(k_p r) \sin 2\theta \right] \cos(k_p z) \end{aligned} \quad (67)$$

and

$$\begin{aligned} P_C = -\rho \{ & \ddot{q}_1^C(t) \left[R \sin\theta - \frac{3\pi R}{16} \sin 2\theta \right] + \\ & + \sum_{p=2,4}^{\infty} \ddot{q}_{1,p}^C(t) \left[I_1(k_p R) \sin\theta - \frac{3\pi}{8} \frac{I_1'(k_p R)}{I_2'(k_p R)} I_2(k_p R) \sin 2\theta \right] \cos(k_p z) \} \end{aligned} \quad (68)$$

respectively. Furthermore, the total force per unit length is

$$f_C = -\frac{m_L}{2} \ddot{q}_1^C(t) - m_L \sum_{p=2,4}^{\infty} \ddot{q}_{1,p}^C(t) \left[\frac{I_1(k_p R)}{R} - \frac{I_2(k_p R)}{R} \frac{I_1'(k_p R)}{I_2'(k_p R)} \right] \cos(k_p z) \quad (69)$$

where the generalized coordinates $q_1^C(t)$ and $q_{1,p}^C(t)$ are computed through the following ordinary differential equations,

$$\ddot{q}_1^C(t) + \omega_{s0}^2 q_1^C(t) = \omega_{s0}^2 [X(t) + \psi_m \Delta(t)] \quad (70)$$

$$\ddot{q}_{1,p}^C(t) + \omega_{sp}^2 q_{1,p}^C(t) = \gamma_p \Delta(t), \quad p = 2, 4, 6, \dots \quad (71)$$

where

$$\omega_{s0}^2 = \frac{3\pi g}{8R} \quad (72)$$

$$\omega_{sp}^2 = \frac{3\pi g k_p}{16} \frac{I_1'(k_p R)}{I_2'(k_p R)} \quad (73)$$

$$\gamma_p = \omega_{s0}^2 \frac{a_p R}{I_2'(k_p R)} \quad (74)$$

Finally, conducting the appropriate integrations in Equation (56), the following equation is obtained from the dynamic equilibrium of the deformable cylinder

$$\left(M'_T - \sum_{p=2,4}^{\infty} M_{sp} \right) \ddot{\Delta} + K_b \Delta + (M_T - M_{s0}) \ddot{X} + M_{s0} \ddot{q}_{1,0}^C + \sum_{p=2,4}^{\infty} M_{sp} \frac{\omega_{sp}^2}{\gamma_p} \ddot{q}_{1,p}^C = 0 \quad (75)$$

where

$$M_T = \int_0^L m_L \psi(z) dz = m_L \psi_m L \quad (76)$$

$$M_{S0} = \int_0^L \frac{m_L}{2} \psi(z) dz = \frac{m_L}{2} \psi_m L \quad (77)$$

$$M_{Sp} = \left(\frac{L}{R} \right) m_L \frac{\gamma_p}{\omega_{Sp}^2} B_p a_p \quad (78)$$

$$M'_T = \left\{ M_{S0} \psi_m + \sum_{p=2,4}^{\infty} M_{Sp} + 2 \left(\frac{L}{R} \right) m_L \sum_{p=2,4}^{\infty} \frac{I_2(k_p R)}{k_p I'_2(k_p R)} a_p^2 \right\} \quad (79)$$

$$a_p = \frac{1}{L} \int_0^L \cos(k_p z) \tilde{\psi}(z) dz \quad (80)$$

$$B_p = I_1(k_p R) - \frac{I'_1(k_p R)}{I'_2(k_p R)} I_2(k_p R) \quad (81)$$

Equation (70) is separated in two parts, so that $q_l^C = q_{lA}^C + q_{lB}^C$ and

$$\ddot{q}_{lA}^C(t) + \omega_{S0}^2 q_{lA}^C(t) = \omega_{S0}^2 X(t) \quad (82)$$

$$\ddot{q}_{lB}^C(t) + \omega_{S0}^2 q_{lB}^C(t) = \omega_{S0}^2 \psi_m \Delta(t) \quad (83)$$

Subsequently, a change of variables is introduced

$$q_{lA}^C = q_g + X \quad (84)$$

$$q_{lB}^C = \psi_m (Q_0 + \Delta) \quad (85)$$

$$q_{l,p}^C = \frac{\gamma_p}{\omega_{Sp}^2} (Q_p + \Delta) \quad (86)$$

and the system of equations (82), (83), (71) and (75), written in terms of the new variables q_g , and Q_0, Q_p ($p = 2, 4, 6, \dots$), takes the following form

$$\ddot{q}_g(t) + \omega_{S0}^2 q_g(t) = -\ddot{X}(t) \quad (87)$$

$$\ddot{Q}_0(t) + \omega_{S0}^2 Q_0(t) = -\ddot{\Delta}(t) \quad (88)$$

$$\begin{aligned} & \vdots \\ \ddot{Q}_p(t) + \omega_{Sp}^2 Q_p(t) &= -\ddot{\Delta}(t) \end{aligned} \quad (89)$$

and

$$\frac{M_{S0}}{M_b} \ddot{q}_g + \frac{M_{S0} \psi_m}{M_b} \ddot{Q}_0 + \sum_{p=2,4}^{\infty} \frac{M_{Sp}}{M_b} \ddot{Q}_p + \left(\frac{M'_T + M_{S0} \psi_m}{M_b} \right) \ddot{\Delta} + \omega_b^2 \Delta = -\frac{M_T}{M_b} \ddot{X} \quad (90)$$

where

$$\omega_b^2 = \frac{K_b}{M_b} \quad (91)$$

and the equation of motion of the container is normalized by M_b , defined as follows:

$$M_b = \int_0^L m_L \psi^2(z) dz \quad (92)$$

The value of M_b can be considered as a generalized mass of the entire liquid.

The system of equations (87) - (90) can be written in matrix form as follows

$$[\mathcal{M}] \ddot{\mathbf{Q}} + [\mathcal{K}] \mathbf{Q} = -\{\mathcal{T}\} \ddot{\mathbf{X}} \quad (93)$$

where

$$[\mathcal{M}] = \begin{bmatrix} 1 & 0 & 0 \dots \dots \dots 0 & 0 \\ 0 & 1 & 0 \dots \dots \dots 0 & 1 \\ 0 & 0 & 1 \dots \dots \dots 0 & 1 \\ \vdots & \vdots & \vdots & \vdots \\ 0 & 0 & 0 \dots \dots \dots 1 & 1 \\ \frac{M_{S0}}{M_b} & \frac{M_{S0}\Psi_m}{M_b} & \left(\frac{M_{S2}}{M_b}\right) \dots \dots \dots \left(\frac{M_{SP}}{M_b}\right) & \left(\frac{(M'_T + M_{S0}\Psi_m)}{M_b}\right) \end{bmatrix} \quad (94)$$

$$[\mathcal{K}] = \begin{bmatrix} \omega_{S0}^2 & 0 & 0 & \dots & 0 \\ 0 & \omega_{S0}^2 & 0 & \dots & 0 \\ 0 & 0 & \omega_{S2}^2 & \dots & 0 \\ \vdots & \vdots & \vdots & \vdots & \vdots \\ 0 & 0 & 0 & \dots \omega_{SP}^2 & 0 \\ 0 & 0 & 0 & \dots & \omega_b^2 \end{bmatrix} \quad (95)$$

$$\{\mathcal{T}\} = \begin{bmatrix} 1 & 0 & 0 & \dots & 0 & \frac{M_T}{M_b} \end{bmatrix}^T \quad (96)$$

$$\mathbf{Q} = \begin{bmatrix} q_g & Q_0 & Q_2 & \dots & Q_P & \Delta \end{bmatrix}^T \quad (97)$$

Equation (93) is in the form of a typical dynamic structural system, with no damping. The case of a damped system will be discussed in a later section of this paper. Finally, considering zero external excitation ($\ddot{\mathbf{X}} = 0$) in equation (93), and assuming a harmonic solution, the following eigenvalue problem is obtained

$$\left[-\omega^2 [\mathcal{M}] + [\mathcal{K}] \right] \mathbf{Q} = 0 \quad (98)$$

and its solution provides the frequencies $\omega_{(i)}$ of the coupled liquid-container problem.

4.3 Application for sinusoidal assumed shape function

Assuming a sinusoidal function $\psi(z)$ for the deformation of the cylinder in the following form,

$$\psi(z) = \sin(\pi z/L) \quad (99)$$

one obtains $\psi_m = 2/\pi$, $M_b = m_L L/2$, $a_p = 2/[\pi(1-p^2)]$

$$\frac{M_{s0}}{M_b} = \frac{2}{\pi} \quad (100)$$

$$\frac{M_{sp}}{M_b} = \frac{16}{\pi^2(1-p^2)} \cdot \frac{1}{k_p R} \left[\frac{I_1(k_p R)}{I_1'(k_p R)} - \frac{I_2(k_p R)}{I_2'(k_p R)} \right], \quad p = 2, 4, 6, \dots \quad (101)$$

so that the equilibrium equation (90) becomes

$$\begin{aligned} \omega_b^2 \Delta + \left(\frac{4}{\pi} \right) \ddot{X} + \left(\frac{2}{\pi} \right) \ddot{q}_g + \left(\frac{2}{\pi} \right)^2 \ddot{Q}_0 + \left(\frac{8}{\pi^2} + \sum_{p=2,4}^{\infty} \frac{16}{\pi^2(1-p^2)^2} \frac{1}{x} \frac{I_1(x)}{I_1'(x)} \right) \ddot{\Delta} \\ + \sum_{p=2,4}^{\infty} \frac{16}{\pi^2(1-p^2)^2} \cdot \frac{1}{x} \left[\frac{I_1(x)}{I_1'(x)} - \frac{I_2(x)}{I_2'(x)} \right] \ddot{Q}_p = 0 \end{aligned} \quad (102)$$

where $x = k_p R$. The above expression results in an interesting mathematical result for the particular case of a long cylinder, as shown in the next paragraph.

4.4 The case of a long cylinder

The response of a long cylinder can be described by the above equations setting $L/R \rightarrow \infty$, or equivalently $x \rightarrow 0$, and the following limits are obtained:

$$\lim_{x \rightarrow 0} \frac{1}{x} \left[\frac{I_1(x)}{I_1'(x)} - \frac{I_2(x)}{I_2'(x)} \right] = \frac{1}{2} \quad (103)$$

$$\lim_{x \rightarrow 0} \frac{1}{x} \frac{I_1(x)}{I_1'(x)} = 1 \quad (104)$$

$$\lim_{x \rightarrow 0} \frac{1}{x} \frac{I_2(x)}{I_2'(x)} = \frac{1}{2} \quad (105)$$

$$\lim_{L/R \rightarrow \infty} \omega_{sp}^2 = \omega_{s0}^2 \quad (106)$$

The rate at which ω_{sp} converges to ω_{s0} in equation (106) is shown in Figure 3. Because of equation (106), equations (88) - (89) become identical, implying that $Q_p \equiv Q_0$ for $p=2,4,6,\dots$, so that the equation of motion of the container (102) becomes

$$\omega_b^2 \Delta + \left(\frac{2}{\pi} \right) \ddot{q}_g + \left(\frac{4}{\pi^2} + \sum_{p=2,4,\dots}^{\infty} \frac{8}{\pi^2(1-p^2)^2} \right) \ddot{Q}_0 + \left(\frac{8}{\pi^2} + \sum_{p=2,4,\dots}^{\infty} \frac{16}{\pi^2(1-p^2)^2} \right) \ddot{\Delta} + \left(\frac{4}{\pi} \right) \ddot{X} = 0 \quad (107)$$

Finally, it can be shown that

$$\frac{8}{\pi^2} + \sum_{p=2,4,\dots}^{\infty} \frac{16}{\pi^2(1-p^2)^2} = 1 \quad (108)$$

and, therefore, the system of equations (93) can be written as follows:

$$\begin{bmatrix} 1 & 0 & 0 \\ 0 & 1 & 1 \\ (2/\pi) & (1/2) & 1 \end{bmatrix} \begin{bmatrix} \ddot{q}_g \\ \ddot{Q}_0 \\ \ddot{\Delta} \end{bmatrix} + \begin{bmatrix} \omega_{s0}^2 & 0 & 0 \\ 0 & \omega_{s0}^2 & 0 \\ 0 & 0 & \omega_b^2 \end{bmatrix} \begin{bmatrix} q_g \\ Q_0 \\ \Delta \end{bmatrix} = - \begin{bmatrix} 1 \\ 0 \\ 4/\pi \end{bmatrix} \ddot{X} \quad (109)$$

This system of equation is identical to the equations of motion obtained by Papaspyrou *et al.* (2004b) through a “physical” model, outlined in the Appendix of the present paper.

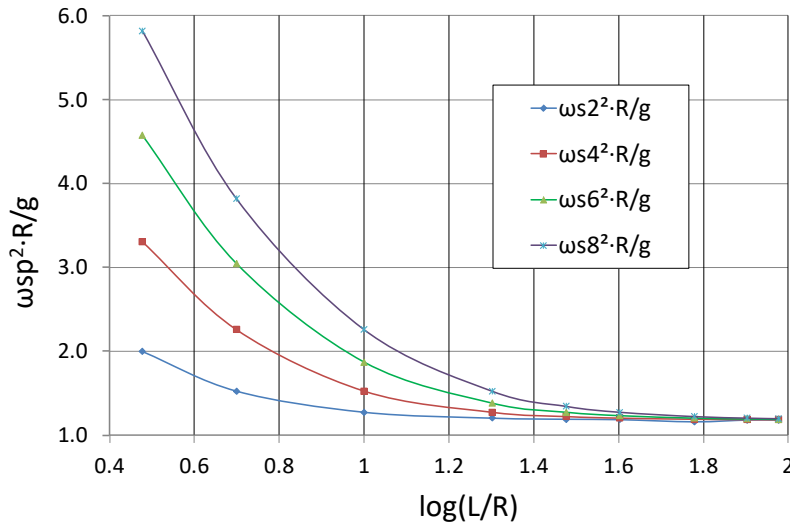


Figure 3: Convergence of ω_{sp} values to the value of ω_{s0} with increasing values of the L/R ratio.

5 RESULTS

The frequencies of the undamped coupled system, computed from equation (98), are shown in Table 1 – Table 4 for four different values of the L/R ratio, and for different values of the truncation size in terms of p in equations (61) and (67). In Figure 4, the first two (lowest) frequencies, together with the last (largest) frequency are plotted with respect to the value of the L/R ratio. One of the two lowest frequencies is always equal to ω_{s_0} , denoted as $\omega_{(1)}$, as indicated by equation (87), and refers to liquid sloshing due to uniform motion of the container, whereas the other frequency, denoted as $\omega_{(2)}$ is equal to ω_{s_0} for L/R values less than 50, but deviates from the value of ω_{s_0} for L/R values greater than 50. Finally, the value of the largest frequency, denoted as ω_{DEF} , corresponds to the vibration of the container. The value of ω_{DEF} is quite large for L/R values less than 20, but reduces rapidly and becomes comparable to the value of ω_{s_0} for L/R values greater than 50, a result also noticed in Table 1 – Table 4.

Truncation Size ($L/R=5$)							
1 ($p=2$)	2 ($p=4$)	3 ($p=6$)	4 ($p=8$)	5 ($p=10$)	6 ($p=12$)	7 ($p=14$)	8 ($p=16$)
1.178093	1.178093	1.178093	1.178093	1.178093	1.178093	1.178093	1.178093
1.178097	1.178097	1.178097	1.178097	1.178097	1.178097	1.178097	1.178097
1.524002	1.524002	1.524002	1.524002	1.524002	1.524002	1.524002	1.524002
269908.84	2.256482	2.256482	2.256482	2.256482	2.256482	2.256482	2.256482
	268551.38	3.045854	3.045854	3.045854	3.045854	3.045854	3.045854
		268364.00	3.817625	3.817625	3.817625	3.817625	3.817625
			268318.85	4.574150	4.574150	4.574150	4.574150
				268304.02	5.322726	5.322726	5.322726
					2682980.72	6.067368	6.067368
						268295.33	6.809995
							268293.92

Table 1: Normalized frequencies of the coupled system ($L/R=5$, $\omega_b^2 R/g = 130949.72$).

Truncation Size ($L/R=10$)							
1 ($p=2$)	2 ($p=4$)	3 ($p=6$)	4 ($p=8$)	5 ($p=10$)	6 ($p=12$)	7 ($p=14$)	8 ($p=16$)
1.178029	1.178029	1.178029	1.178029	1.178028	1.178028	1.178028	1.178028
1.178097	1.178097	1.178097	1.178097	1.178097	1.178097	1.178097	1.178097
1.272067	1.272067	1.272067	1.272067	1.272067	1.272067	1.272067	1.272067
16619.09	1.523980	1.523980	1.523980	1.523980	1.523980	1.523980	1.523980
	16511.97	1.870291	1.870291	1.870291	1.870291	1.870291	1.870291
		16494.72	2.256435	2.256435	2.256435	2.256435	2.256435
			16490.10	2.652232	2.652232	2.652232	2.652232
				16488.48	3.045768	3.045768	3.045768
					16487.80	3.434083	3.434083
						16487.48	3.817490
							16487.31

Table 2: Normalized frequencies of the coupled system ($L/R=10$, $\omega_b^2 R/g = 8184.3575$).

Truncation Size (L/R=40)							
1 (p=2)	2 (p=4)	3 (p=6)	4 (p=8)	5 (p=10)	6 (p=12)	7 (p=14)	8 (p=16)
1.157486	1.157411	1.157403	1.157401	1.157401	1.157400	1.157400	1.157400
1.178097	1.178097	1.178097	1.178097	1.178097	1.178097	1.178097	1.178097
1.183255	1.183254	1.183253	1.183253	1.183253	1.183253	1.183253	1.183253
65.763792	1.202053	1.202053	1.202053	1.202053	1.202053	1.202053	1.202053
	65.301275	1.231644	1.231644	1.231644	1.231644	1.231644	1.231644
		65.217863	1.272075	1.272075	1.272075	1.272075	1.272075
			65.192507	1.322542	1.322542	1.322542	1.322542
				65.182417	1.382065	1.382065	1.382065
					65.177679	1.449583	1.449583
						65.175189	1.524002
							65.173770

Table 3: Normalized frequencies of the coupled system ($L/R=40$, $\omega_b^2 R/g = 31.97014$).

Truncation Size (L/R=90)							
1 (p=2)	2 (p=4)	3 (p=6)	4 (p=8)	5 (p=10)	6 (p=12)	7 (p=14)	8 (p=16)
0.637939	0.635403	0.634943	0.634804	0.634748	0.634722	0.634709	0.634701
1.178097	1.178097	1.178097	1.178097	1.178097	1.178097	1.178097	1.178097
1.178976	1.178966	1.178962	1.178960	1.178958	1.178957	1.178975	1.178975
3.746990	1.181745	1.181683	1.181653	1.181635	1.181622	1.182357	1.182357
	3.734910	1.186583	1.186442	1.186366	1.186317	1.187718	1.187718
		3.732715	1.193527	1.193298	1.193169	1.195174	1.195174
			3.732040	1.193298	1.202246	1.204704	1.204704
				3.731768	1.213660	1.216271	1.216271
					3.731638	1.229829	1.229829
						3.731568	1.245328
							3.731527

Table 4: Normalized frequencies of the coupled system ($L/R=90$, $\omega_b^2 R/g = 1.0048244$).

Another issue related to the frequencies refers to the value of the largest frequency ω_{DEF} of the coupled system, which may offer valuable information on the dynamic behavior of the container. Considering the motion of the container as a generalized single-degree-of-freedom system, one may write the vibration frequency of the moving container in terms of its stiffness K_b given in equation (57), and a generalized mass \mathbf{M} which represents the part of liquid mass moving with the container, as follows:

$$\omega_{DEF}^2 = \frac{K_b}{\mathbf{M}} \quad (110)$$

Combining equations (110) and (91), one obtains a simple expression for the generalized liquid mass \mathbf{M} that follows the motion of the container:

$$\frac{\mathbf{M}}{M_b} = \left(\frac{\omega_b}{\omega_{DEF}} \right)^2 \quad (111)$$

Expression (111) shows that the value of \mathbf{M} depends on the L/R ratio and it is plotted in Figure 5, normalized by the value of M_b , defined in equation (92). The \mathbf{M}/M_b ratio expresses the part of total liquid mass that follows the motion of the

container, whereas the remaining part of the liquid is associated with sloshing. The results in Figure 5 show that for L/R values less than 40, the liquid mass is divided in two equal parts: one associated with sloshing and one that follows the motion of the container. This is a result consistent with the one presented in Papaspyrou *et al.* (2004b).

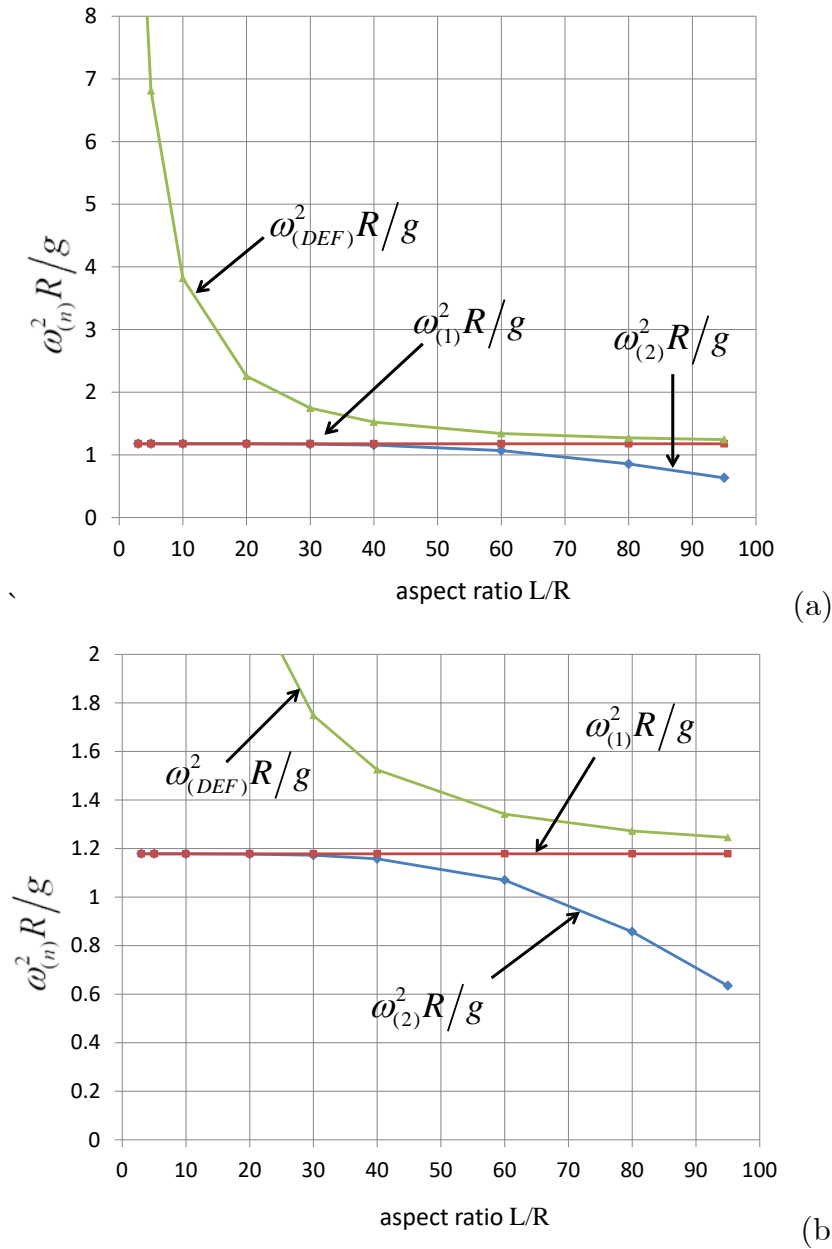


Figure 4: Variation of the first two frequencies and the last (largest) frequency in terms of the L/R ratio; (a) entire range of frequencies and (b) detail of the graph.

For larger values of the aspect ratio L/R , the value of the \mathbf{M}/M_b ratio decreases below the value of 0.5, so that less than half of liquid mass follows the motion of the container, while the mass associated with sloshing becomes larger. This decrease of the \mathbf{M}/M_b ratio is attributed to the values of ω_{DEF} and ω_b , both associated with the deformation of the container; their values are significantly low for very long containers and comparable with the value of the sloshing frequency ω_{s0} (see Figure 4 and Table 4). In such a case, there is coupling between the container motion and sloshing motion, so that the liquid mass associated with sloshing is increased, whereas the corresponding mass that follows the motion of the container is decreased, as indicated by the \mathbf{M}/M_b ratio.

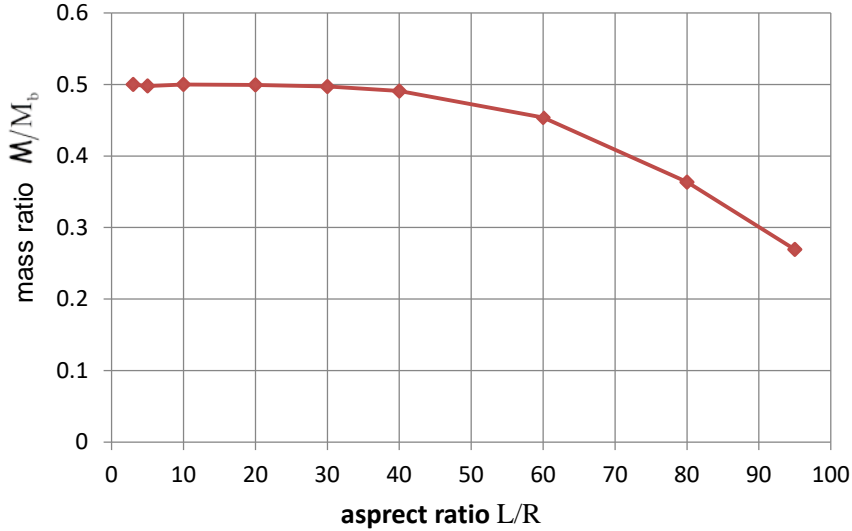


Figure 5: Ratio of generalized mass \mathbf{M} , representing the liquid mass moving with the container, over generalized total liquid mass M_b , in terms of the L/R aspect ratio.

Results for the response of the liquid-vessel system are also obtained for external excitation in the form of the accelerogram shown in Figure 6, from the Kobe 1995 earthquake, a serious seismic event. The vessel under consideration has radius R equal to 1 meter, thickness h equal to 2 cm, and it is considered half-full with liquid of density equal to 1000 kg/m^3 . To obtain realistic results for this seismic excitation,

appropriate damping terms are introduced in equations (87) – (90), resulting to the addition of a damping term, proportional to $\dot{\mathbf{Q}}$ in the equations of motion, so that:

$$[\mathcal{M}]\ddot{\mathbf{Q}} + [\mathcal{C}]\dot{\mathbf{Q}} + [\mathcal{K}]\mathbf{Q} = -\{\mathcal{T}\}\ddot{\mathbf{X}} \quad (112)$$

where the damping matrix $[\mathcal{C}]$ is considered in the following diagonal form:

$$[\mathcal{C}] = \begin{bmatrix} 2\xi_{s0}\omega_{s0} & 0 & 0 & 0 & 0 & 0 \\ 0 & 2\xi_{s0}\omega_{s0} & 0 & 0 & 0 & 0 \\ 0 & 0 & 2\xi_{s1}\omega_{sp1} & 0 & 0 & 0 \\ \vdots & \vdots & \vdots & \ddots & \vdots & \vdots \\ 0 & 0 & 0 & 0 & 2\xi_{sn}\omega_{spn} & 0 \\ 0 & 0 & 0 & 0 & 0 & 2\xi_b\omega_b \end{bmatrix} \quad (113)$$

In the present analysis, the values of damping coefficients ξ_{s0} , ξ_{sj} ($j=1,2,\dots,n$), ξ_b are equal to 0.02. The integration of the system of equations (112) is performed using Newmark's algorithm with constants $\beta=1/4$ and $\gamma=1/2$, in an in-house program within Matlab environment. Results for the container under consideration are reported in Figure 7 and Figure 8 for two values of the aspect ratio L/R , namely 10 and 40. The results indicate that the aspect ratio has a significant effect on the response of the container.

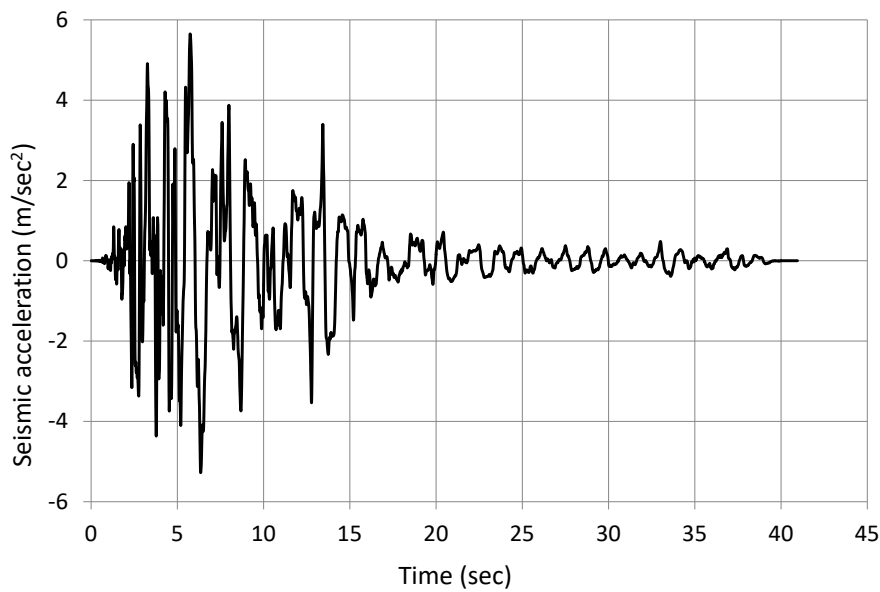


Figure 6: Seismic motion (accelerogram) from Kobe 1995 earthquake.

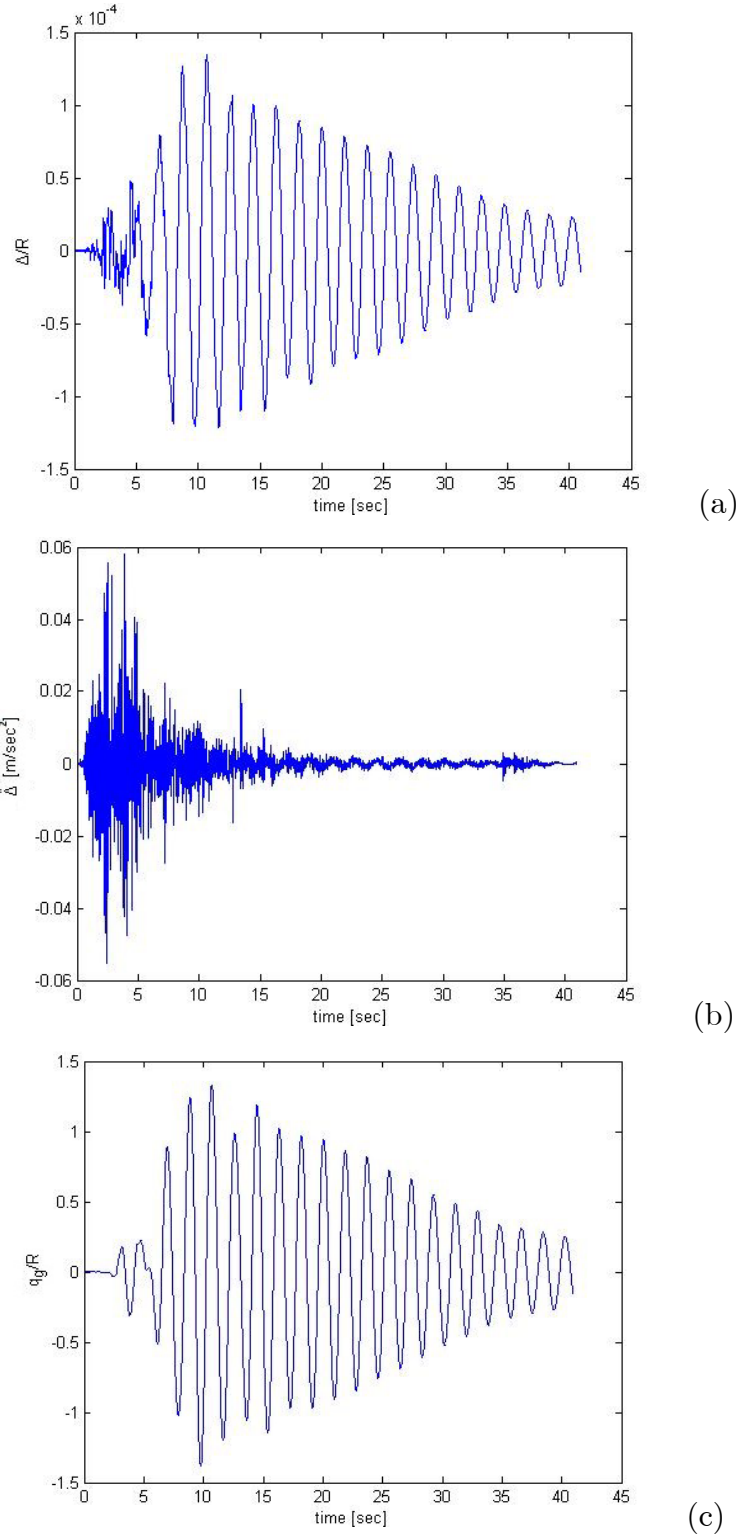


Figure 7: Response of the coupled liquid-container system to Kobe 1995 earthquake ($L/R = 10$); (a) container displacement Δ ; (b) container acceleration $\ddot{\Delta}$; (c) sloshing generalized coordinate q_g .

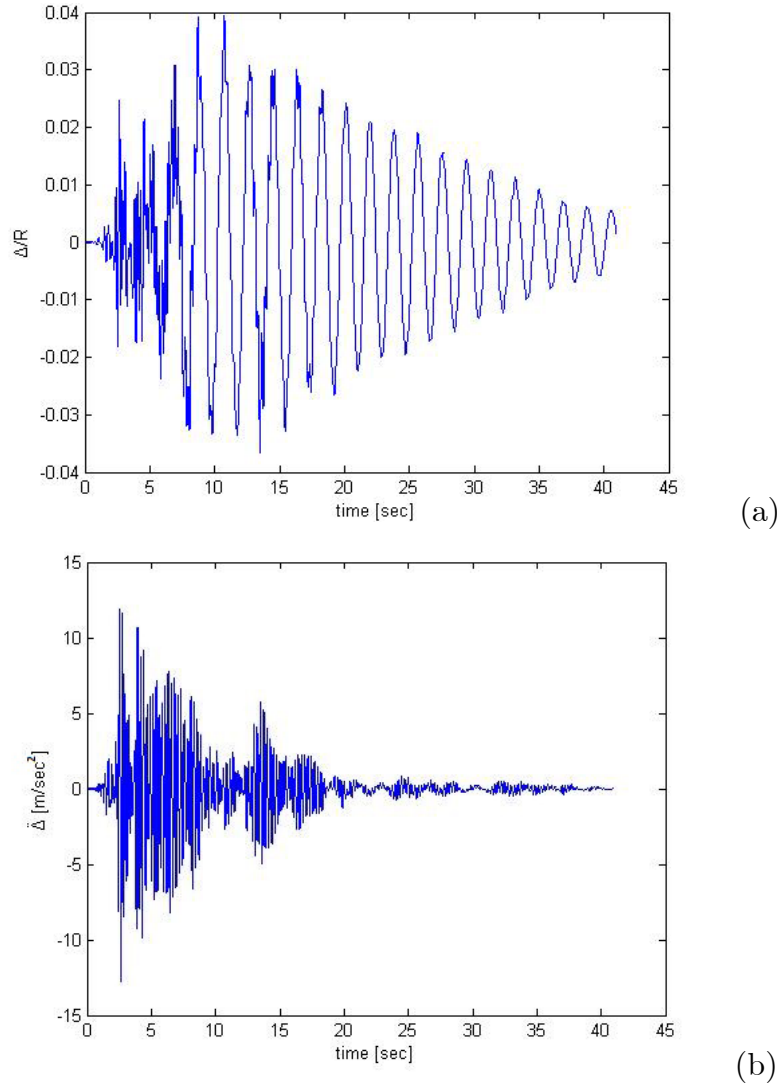


Figure 8: Response of the coupled liquid-container system to Kobe 1995 earthquake ($L/R = 40$); (a) container displacement Δ ; (b) container acceleration $\ddot{\Delta}$.

6 SUMMARY AND CONCLUSIONS

Motivated by the analysis of horizontal cylindrical vessels under seismic excitation, the coupled response of deformable half-full liquid containers of horizontal-cylindrical shape under external excitation has been examined, through an analytical methodology, expanding the velocity potential in terms of arbitrary time functions. Full coupling between sloshing and wall deformation is considered, assuming a beam-type assumed-shape function for the cylinder deformation.

Using a two-term truncation of the series solution in the transverse direction, an elegant mathematical solution is obtained for the transient problem, which results in a system of ordinary differential equations. For long cylinders and assuming a sinusoidal shape function for cylinder deformation, it is demonstrated that the present solution is identical to the solution proposed by Papaspyrou *et al.* (2004b), obtained through a “physical” model.

Results are obtained for containers of different aspect ratio, in terms of the natural frequencies of the coupled system, and the system response under external excitation in the form of a severe seismic input. The numerical results indicate that for cylinders with small value of aspect ratio L/R , the principal “convective” natural frequencies are significantly smaller than the natural frequency associated with the deformation of the container, and the corresponding “convective” liquid mass is half of the total liquid mass. For long cylinders (large value of L/R), the “deformation” natural frequency value is close to the value of the principal “convective” natural frequencies, implying coupling between the motion of the container and sloshing motion, so that the corresponding “convective” liquid mass becomes more than half of the total liquid mass.

ACKNOWLEDGEMENT

The authors would like to thank Dr. Vasilis Kanakoudis, Associate Professor of Civil Engineering, University of Thessaly, for his valuable support during this work.

REFERENCES

- [1] Budiansky, B. (1960), “Sloshing of Liquids in Circular Canals and Spherical Tanks”, *Journal of Aerospace Sciences*, Vol. 27, Number 3, pp. 161-173.
- [2] Moiseev, N. N. and Petrov, A. A. (1966), “The Calculation of Free Oscillations of a Liquid in a Motionless Container”, *Advances in Applied Mechanics*, Vol. 9, pp. 91-154.

- [3] Fox, D. W. and Kutler, J. R. (1981), “Upper and Lower Bounds for Sloshing Frequencies by Intermediate Problems”, *Journal of Applied Mathematics and Physics*, Vol. 32, pp. 667-682.
- [4] Fox, D. W. and Kutler, J. R. (1983), “Sloshing Frequencies”, *Journal of Applied Mathematics and Physics*, Vol. 34, pp. 669-696.
- [5] McIver, P. (1989), “Sloshing Frequencies for Cylindrical and Spherical Containers Filled to an Arbitrary Depth”, *Journal of Fluid Mechanics*, Vol. 201, pp. 243-257.
- [6] McIver, P. and McIver, M. (1993), “Sloshing Frequencies of Longitudinal Modes for a Liquid Contained in a Trough”, *Journal of Fluid Mechanics*, Vol. 252, pp. 525-541.
- [7] Zhou, H., Li, J. F. and Wang, T. S. (2008), “Simulation of liquid sloshing in curved-wall containers with arbitrary Lagrangian–Eulerian method”, *International Journal of Numerical Methods in Fluids*, Vol. 57, pp. 437–452.
- [8] Faltinsen, O. M., and Timokha, A. N. (2009), *Sloshing*, Cambridge University Press, New York, NY.
- [9] Faltinsen, O. M., and Timokha, A. N. (2010), “A multimodal method for liquid sloshing in a two dimensional circular tank”, *Journal of Fluid Mechanics*, Vol. 665, pp. 457–479.
- [10] Kolaei, A., Rakheja, S., Richard, M. J. (2014a), “Range of applicability of the linear fluid slosh theory for predicting transient lateral slosh and roll stability of tank vehicles”, *Journal of Sound and Vibration*, Vol. 333, pp. 263–282.
- [11] Kolaei, A., Rakheja, S., Richard, M. J. (2014b), “Effects of tank cross-section on dynamic fluid slosh loads and roll stability of a partly-filled tank truck”, *European Journal of Mechanics B/Fluids*, Vol. 46. pp. 46–58.
- [12] Kobayashi, N., Mieda, T., Shibata, H. and Shinozaki, Y. (1989), “A Study of the Liquid Slosh Response in Horizontal Cylindrical Tanks”, *Journal of Pressure Vessel Technology*, ASME, Vol. 111, pp. 32-38.
- [13] Patkas, L. A. and Karamanos, S. A. (2007), “Variational Solutions of Liquid Sloshing in Horizontal-Cylindrical and Spherical Containers”, *Journal of Engineering Mechanics*, ASCE, Vol. 133, No. 6, pp. 641-655.

- [14] Karamanos, S. A., Papaprokopiou, D., and Platyrrachos, M. A. (2009), “Finite Element Analysis of Externally-Induced Sloshing in Horizontal-Cylindrical and Axisymmetric Industrial Vessels”, *Journal of Pressure Vessel Technology*, ASME, Vol. 131, No. 5, Article Number: 051301.
- [15] Malhotra, P. K., Nimse, P. and Meekins, M. (2014), “Seismic Sloshing in a Horizontal Liquid-Storage Tank”, *Structural Engineering International*, Vol. 24, No. 4, pp. 466-473.
- [16] Evans, D. V., and Linton, C. M. (1993), “Sloshing frequencies”, *Quarterly Journal of Mechanics and Applied Mathematics*, Vol. 46, Pt. 1, pp. 71-87.
- [17] Papaspyrou, S., Valougeorgis, D. and Karamanos, S. A. (2004a), “Sloshing effects in half-full horizontal cylindrical vessels under longitudinal excitation”, *Journal of Applied Mechanics*, ASME, Vol. 71, No. 2, pp. 255-265.
- [18] Papaspyrou, S., Karamanos, S. A. and Valougeorgis, D. (2004b), “Response of Half Full Horizontal Cylinders Under Transverse Excitation”, *Journal of Fluids and Structures*, Vol. 19, No. 7, pp. 985-1003.
- [19] Karamanos, S. A., Patkas, L. A. and Platyrrachos, M. A. (2006), “Sloshing Effects on the Seismic Design of Horizontal-Cylindrical and Spherical Industrial Vessels”, *Journal of Pressure Vessel Technology*, ASME, Vol. 128, No. 3, pp. 328-340.
- [20] Hasheminejad, S. M. and Aghabeigi, M. (2009), “Liquid sloshing in half-full horizontal elliptical tanks”, *Journal of Sound and Vibration*, Vol. 324, pp. 332–349.
- [21] Hasheminejad, S. M. and Aghabeigi, M. (2011), “Transient sloshing in half-full horizontal elliptical tanks under lateral excitation”, *Journal of Sound and Vibration*, Vol. 330, pp. 3507–3525.
- [22] Hasheminejad, S. M. and Aghabeigi, M. (2012), “Sloshing characteristics in half-full horizontal elliptical tanks with vertical baffles”, *Applied Mathematical Modelling*, Vol. 36, pp. 57–71.
- [23] Veletsos, A. S. and Yang, J. Y. (1977), “Earthquake Response of Liquid Storage Tanks”, *2nd Engineering Mechanics Conference*, ASCE, Raleigh, NC, pp. 1-24.

- [24] Fisher, F. D. (1979), “Dynamic Fluid Effects in Liquid-Filled Flexible Cylindrical Tanks”, *Earthquake Engineering and Structural Dynamics*, Vol. 7, pp. 587-601.
- [25] Haroun, M. A. and Housner, G. W. (1981), “Earthquake Response of Deformable Liquid Storage Tanks”, *Journal of Applied Mechanics*, ASME, Vol. 48, pp. 411-417.
- [26] Natsiavas, S. (1988), “An Analytical Model for Unanchored Fluid-Filled Tanks Under Base Excitation”, *Journal of Applied Mechanics*, ASME, Vol. 55, pp. 648-653.
- [27] Gupta, R. K. (1995), “Sloshing In Shallow Cylindrical Tanks”, *Journal of Sound and Vibration*, Vol. 180. No.3, pp. 297-304.
- [28] Fischer, F. D. and Rammerstorfer, F. G. (1999), “A refined analysis of sloshing effects in seismically excited tanks”, *International Journal of Pressure Vessels and Piping*, Vol. 76, pp. 693–709.

APPENDIX. SIMPLIFIED MODEL FOR VESSEL-LIQUID INTERACTION

It is possible to develop a simplified model that accounts for vessel-liquid interaction, using a simplified “physical” approach. The model is based on the two-dimensional sloshing solution for the non-deformable half-full container and an assumed shape function, as in equation (1), resulting in a system of equations identical to (109). The formulation of this methodology is described in detail in [17], and it is outlined herein for the sake of completeness.

The sloshing problem of the non-deformable container under transverse excitation can be described mathematically by equations (2) - (5), setting $\Delta = 0$. Solution of this problem is sought expressing the liquid potential in the following form:

$$\Phi(r, \theta, t) = \dot{X}(t) r \sin \theta + \bar{\varphi}(r, \theta, t) \quad (114)$$

where the first term on the right-hand side of equation (114) is a potential that satisfies the non-homogeneous boundary condition of the moving container, and $\bar{\varphi}$ is a potential associated with sloshing. Expressing $\bar{\varphi}$ as follows

$$\varphi(r,\theta,t) = \dot{\alpha}_1 r \sin\theta + \dot{\alpha}_2 r^2 \sin 2\theta \quad (115)$$

one obtains

$$\ddot{\alpha}_1 + \left(\frac{3\pi g}{8R} \right) \alpha_1 = -\ddot{X} \quad (116)$$

$$\alpha_2 = - \left(\frac{3\pi}{16R} \right) \alpha_1 \quad (117)$$

and the total hydrodynamic force per unit length on the cylinder wall along its length is

$$f = -m_L \ddot{X} - m_s \ddot{\alpha}_1 \quad (118)$$

The above solution can be used as a basis for the developing a simplified three-dimensional model for the deformable container. Substituting in equation (116) the excitation function $X(t)$ with function $X(t) + \psi(z)\Delta(t)$,

$$\ddot{\alpha}_1 + \omega_{s0}^2 \alpha_1 = -\ddot{X} + \psi \ddot{\Delta} \quad (119)$$

and decomposing the sloshing motion in two parts, one associated with the external excitation and one with the deformation of the container setting

$$\alpha_1 = \psi(z) \alpha_s + \alpha_g \quad (120)$$

one obtains

$$\ddot{\alpha}_g + \omega_{s0}^2 \alpha_g = -\ddot{X} \quad (121)$$

$$\ddot{\alpha}_s + \omega_{s0}^2 \alpha_s = -\ddot{\Delta} \quad (122)$$

and the force per unit length becomes:

$$f(z,t) = -m_s \ddot{\alpha}_g - m_L \ddot{X} - m_s \psi(z) \ddot{\alpha}_s - m_L \psi(z) \ddot{\Delta} \quad (123)$$

Finally, using the weak form of the cylinder equation of motion (51), one obtains

$$M_s \ddot{q}_g + M_T \ddot{X}_g + M'_s \ddot{q} + M'_T \ddot{\Delta} + K_b \Delta = 0 \quad (124)$$

The system of equations (121), (122) and (124) in terms of $\alpha_g, \alpha_s, \Delta$ is identical to the one of equation (109) corresponding to the limit case of infinitely long cylinder ($L/R \rightarrow \infty$).